NaV1.5 enhances breast cancer cell invasiveness by increasing NHE1-dependent H+ efflux in caveolae

L Brisson, L Gillet, S Calaghan, P Besson, Jean-Yves Le Guennec, S Roger, J. Goré

HAL Id: hal-02908089

https://hal.umontpellier.fr/hal-02908089

Submitted on 20 Aug 2020

Na$_V$1.5 ENHANCES BREAST CANCER CELL INVASIVENESS BY INCREASING NHE1-DEPENDENT H$^+$ EFFLUX IN CAVEOLAE

Lucie BRISSON[1], Ludovic GILLET[1], Sarah CALAGHAN[2], Pierre BESSON[1], Jean-Yves LE GUENNEC[3], Sébastien ROGER[1#] & Jacques GORE[1#]

# both authors contributed equally to the work

[1] Inserm U921, Nutrition, Croissance et Cancer ; Université François Rabelais, Faculté de Médecine, 10 Boulevard Tonnellé, 37032 Tours, France

[2] Institute of systems and membrane biology, University of Leeds, United Kingdom

[3] Inserm U637 Physiopathologie cardiovasculaire, Université Montpellier-2, 371 avenue du Doyen Gaston Giraud, 34295 Montpellier Cedex 05

Correspondence to:

Sébastien Roger, Inserm U921, 10 Boulevard Tonnellé, 37032 Tours (France), (+33) 2 47 36 61 30, Fax: (+33) 2 47 36 62 26

Email: sebastien.roger@univ-tours.fr

Running title: Na$_V$1.5 promotes NHE1-dependent invasiveness

Number of words: 2,403

Abstract

Na$_V$1.5 sodium channels enhance the invasiveness of breast cancer cells through the acidic-dependent activation of cysteine cathepsins. Here we showed that the Na$^+$/H$^+$ exchanger type 1 (NHE1) was an important regulator of H$^+$ efflux in breast cancer cells MDA-MB-231 and that its activity was increased by Na$_V$1.5. Na$_V$1.5 and NHE1 were colocalized in membrane rafts containing caveolin-1. The inhibition of Na$_V$1.5 or NHE1 induced a similar reduction in cell invasiveness and extracellular matrix degradation; no additive effect was observed when they were simultaneously inhibited. Our study suggests that Na$_V$1.5 and NHE1 are functionally coupled and enhance the invasiveness of cancer cells by increasing H$^+$ efflux.

Key words: cancer, caveolae, invasion, Na$^+$/H$^+$ exchanger, voltage-gated sodium channels

Introduction

Breast cancer is the primary cause of death by cancer in women worldwide mostly as a consequence of the appearance of metastases (Parkin et al., 2005). The development of metastases consists of a complex series of events. One key step is the acquisition by cancer cells of an invasive potency, mainly relying on the capacity to degrade basement membranes and extracellular matrices (Gupta & Massague, 2006) by various proteases such as matrix metalloproteinases (Egeblad & Werb, 2002) or cysteine cathepsines (Mohamed & Sloane, 2006). We and others have shown that voltage-gated sodium channels (Na_V) are abnormally expressed in cancer cells of epithelial origin and associated with cancer progression (Diaz et al., 2007; Fraser et al., 2005; Laniado et al., 1997; Roger et al., 2003; Roger et al., 2006; Roger et al., 2007). In the highly invasive MDA-MB-231 breast cancer cell line, $Na_V1.5$ activity enhances extracellular matrix invasion by increasing the activity of acidic cysteine cathepsins B and S through an acidification of the pericellular microenvironment (Gillet et al., 2009). In this study, we investigated the potential pH regulators involved in the Na_V-dependent invasiveness of MDA-MB-231 breast cancer cells. We found that the Na^+/H^+ exchanger type 1 (NHE1) is the central regulator of intracellular pH and that its activity is enhanced by the function of $Na_V1.5$. These two proteins were colocalized in the membrane fractions which contain caveolae.

Results and Discussion

In a recent study in highly invasive MDA-MB-231 breast cancer cells, we have shown that $Na_V1.5$ activity is responsible for the enhancement of extracellular matrix invasion through perimembrane acidification, which consequently promotes the activity of acidic cathepsins (Gillet et al., 2009). In order to determine the pH regulators that are involved in this phenomenon, we first analysed the effect of various inhibitors and solutions on H^+ efflux. Proton effluxes were assessed in MDA-MB-231 cells that were acidified by NH_4Cl pulse-wash then resuspended in a sodium free solution. The subsequent addition of 130 mM NaCl generated H^+ effluxes and was used as a control condition. The Na^+/H^+ exchangers inhibitor EIPA reduced H^+ efflux by approximately 90% while the V-ATPase inhibitor bafilomycin had no effect (Fig. 1A and B). Resuspending the cells in Na_2SO_4 showed no difference compared to NaCl (Fig. 1C). These results indicate that H^+ efflux was dependent on Na^+ and not on Cl^-. This was further demonstrated in absence of sodium (no addition of NaCl, or substitution by CholineCl or N-methyl-D-glucamine). Bicarbonates were ineffective in regulating H^+ efflux in these conditions. This was confirmed by the use of 4,4'-diisothiocyanato-stilbene-2,2'-disulfonic acid (DIDS), an inhibitor of anionic exchangers (Fig. 1C). Taken together these results indicate a prominent role for Na^+/H^+ exchangers (NHE) in controlling H^+ efflux. The IC_{50} of EIPA on H^+ efflux was 0.11 ± 0.02 μM (Suppl. Fig. 1B). We tested the effect of siRNA directed against NHE1 mRNA (Fig. 1D, Suppl. Fig. 1B). Silencing NHE1 led to a 60% reduction of H^+ efflux compared to the control condition (siCTL, Fig. 1E). EIPA induced a small but significant additional reduction in H^+ efflux. We analysed NHE1 and voltage-gated sodium channel $Na_V1.5$ mRNA expression in non-cancer human breast epithelial cells MCF-10A, and in MDA-MB-231 and MCF-7 breast cancer cells (Fig. 2A). All cell lines expressed mRNA for NHE1 at comparable levels. As previously reported (Fraser et al., 2005; Gillet et al., 2009) the highly invasive MDA-MB-231 breast cancer cell line expresses high levels of mRNA for $Na_V1.5$, while

the poorly invasive MCF-7 cell line showed a weak expression and the non-cancer cell line MCF-10A no expression at all. In line with these findings, only MDA-MB-231 cells exhibited voltage-gated sodium currents (Fig. 2B). Silencing RNA directed against $Na_V1.5$ mRNA ($siNa_V1.5$, Suppl. Fig. 1C) were used to inhibit the expression of $Na_V1.5$. Figure 2C shows the specific effect on $Na_V1.5$ protein expression, with no change in NHE1 expression. Tetrodotoxin (TTX, 30µM) and $siNa_V1.5$ abolished I_{Na} but EIPA did not (Fig. 2D). We then questioned whether the functioning of $Na_V1.5$ could modify NHE1 activity. Here again EIPA reduced H^+ efflux in MDA-MB-231 cells by approximately 90%. The abolition of I_{Na}, using either TTX or $siNa_V1.5$, was responsible for a significant reduction of H^+ efflux. Furthermore, TTX did not induce a supplementary reduction in H^+ efflux when co-applied with EIPA (Fig. 2E). This indicated that $Na_V1.5$ could promote H^+ efflux through NHE. Conversely, TTX had no effect in regulating H^+ efflux from MCF-7 cells (Fig. 2F) which are devoid of I_{Na} (Fig. 2B).

Silencing NHE1 had no effect on the $Na_V1.5$ current-voltage relationship (Suppl. Fig.1E) and did not modify the window of voltage of I_{Na} (Suppl. Fig. 1F). This window of voltage is thought to regulate cell invasiveness because it encompasses the membrane potential of the cells, at which $Na_V1.5$ is active and thus allows a persistent sodium entry (Gillet et al., 2009; Roger et al., 2003). The inhibition of either NHE1, by the use of siNHE1 or EIPA, or $Na_V1.5$, by $siNa_V1.5$ or TTX, produced the same reduction of cell invasiveness by nearly 35% (Fig. 3A). Importantly, the co-inhibition of NHE1 and $Na_V1.5$ with either siNHE1 plus TTX or $siNa_V1.5$ plus EIPA had no supplementary effect. Experiments were then performed to understand how $Na_V1.5$ and NHE1 influenced the matrix degradation. To do so, we used DQ-gelatin which releases fluorescent products after proteolytic cleavage by gelatinases, in a three-dimensional matrix of Matrigel®. The gelatinolytic activity was mainly distributed at the pericellular zone of cancer cells (Fig. 3B). Culture with TTX reduced gelatinolysis of the pericellular matrix (~63% reduction in fluorescence intensity) to the same extent as previously reported (Gillet et al., 2009), confirming the regulatory role of $Na_V1.5$ in extracellular gelatinolysis (Fig. 3B and 3C). The use of EIPA reduced matrix

degradation to the same extent as the use of TTX, and the simultaneous application of TTX and EIPA induced no supplementary effect. This absence of additive effect on cell invasiveness and on gelatinolytic activity when NHE1 and $Na_V1.5$ were simultaneously inhibited suggests that they are both involved in the same pH-dependent invasiveness regulatory pathway. We then explored their cellular localization. NHE1 and $Na_V1.5$ were found to colocalize in the plasma membrane of cancer cells grown on Matrigel® (Fig. 4A). We also conducted membrane fractionations by ultracentrifugation on sucrose gradient and found that both NHE1 and $Na_V1.5$ were located in caveolin-1-containing lipid rafts (Fig. 4B).

$Na_V1.5$ channels have been found in the highly metastatic MDA-MB-231 breast cancer cells and in high grade breast cancer biopsies but not in non-cancer or low grade cancer biopsies (Fraser et al., 2005; Roger et al., 2003). These channels have been associated with the invasive properties of cancer cells by enhancing the activity of extracellular cysteine cathepsins B and S, through a pericellular acidification (Gillet et al., 2009). The importance of an acidic tumour microenvironment for cancer cell invasiveness and malignant progression is well established (Kraus & Wolf, 1996; Martinez-Zaguilan et al., 1996; Moellering et al., 2008). The activation of acidic gelatinolytic cathepsins, mainly cathepsin B, is known to be critical in these effects (Bourguignon et al., 2004; Giusti et al., 2008; Rozhin et al., 1994). Among all pH regulators, the ubiquitous Na^+/H^+ exchanger NHE1 has drawn substantial attention in the field of cancer research, allowing cancer cells to adapt to their high metabolic H^+ production (Gatenby et al., 2007). Indeed it has been shown to play a predominant role in extracellular acidification of tumour cells (Bourguignon et al., 2004) and also to be involved in their invasive process (Busco et al., 2010; Cardone et al., 2005; Stock & Schwab, 2009). In this study, we showed for the first time evidence that $Na_V1.5$ channels, abnormally expressed in breast cancer cells, functionally interact with NHE1 in caveolae to enhance its H^+-efflux activity and consequently promote acidic-dependent invasion of the extracellular matrix. Caveolae have been shown to contain NHE1 in other types of cells (Tekpli et al., 2008) and, independently, to be involved in breast cancer cell invasiveness (Yamaguchi et al., 2009). Recently,

it has been shown that NHE1 is localized in invadopodia where it is responsible for an extracellular acidification and the degradation of the extracellular matrix (Busco et al., 2010). Our study brings a new mechanistic explanation for caveolae involvement in cancer cell invasiveness. It demonstrates for the first time that $Na_V1.5$ channels and NHE1 antiporters are partners in cancer cell invasiveness, which might primarily occur after acidic proteases-dependent matrix proteolysis on the extracellular side of caveolae. The relationship between these proteins and the dynamics of their interactions could be even more critical in membrane areas directly involved in matrix degradation such as invadopodia.

Materials and Methods

Inhibitors and chemicals - Tetrodotoxin (TTX) was purchased from Latoxan (France) and was prepared in pH-buffered physiological saline solution at pH 7.4. Fluorescent probes and antibodies were purchased from Invitrogen (France). 5-(N-ethyl-N-isopropyl) amiloride (EIPA) and other drugs and chemicals were purchased from Sigma-Aldrich (France).

Cell culture - Human breast cancer cell lines MDA-MB-231 and MCF-7 were cultured in Dulbecco's modified Eagle's medium (DMEM) supplemented with 5% FCS. The normal mammary epithelial cell line MCF-10A was cultured in DMEM/Ham's F-12, 1:1 mix containing 5% horse serum, insulin (10 µg/mL), epidermal growth factor (20 ng/mL), hydrocortisone (0.5 µg/mL), and 100 ng/mL cholera toxin. Cells were grown at 37°C in a humidified 5% CO_2 incubator.

Cell line RNA extraction, Reverse Transcription and PCR - Total RNA were extracted using RNAgents® Total RNA Isolation System (Promega, France), then reverse-transcribed with a RT kit in presence of random hexamers pd(N)$_6$ 5'-Phosphate (GE Healthcare, France). Quantitative (real time) PCR experiments were performed in triplicate as already described (Gillet et al., 2009). Alternatively, PCR products were analyzed by electrophoresis in a 2% agarose gel containing ethidium bromide, and visualized by UV trans-illumination (Gel Doc 2000 system, Bio Rad).

SiRNA transfection protocol –Cells were transfected using Lipofectamine RNAi max (Invitrogen, France) with 20 nM siRNA directed against SCN5A mRNA (siNa$_V$1.5), and 10 nM against NHE1 mRNA (siNHE1) or scramble siRNA-A as a control (siCTL), all purchased from Tebu-Bio (France).

Electrophysiology - Patch pipettes were pulled from borosilicate glass to a resistance of 4-6 MΩ. Currents were recorded, in whole-cell configuration, under voltage-clamp mode at room temperature using an Axopatch 200B amplifier (Axon Instrument, USA). Cell capacitance and series resistance were electronically compensated by about 60%. Na$^+$ currents (I_{Na}) were studied as

already described (Gillet et al., 2009) and amplitudes were expressed as current density (pA/pF). The Physiological Saline Solution (PSS) had the following composition (in mM): NaCl 140, KCl 4, $MgCl_2$ 1, $CaCl_2$ 2, D-Glucose 11.1, and HEPES 10, adjusted to pH 7.4. The intrapipette solution had the following composition (in mM) : K-Glutamate 125, KCl 20, $CaCl_2$ 0.37, $MgCl_2$ 1, Mg-ATP 1, EGTA 1, HEPES 10, adjusted to pH 7.2.

Migration and in vitro Invasion Assay – Cell migration and invasiveness were analysed as previously described (Gillet et al., 2009) in 24-well plates receiving cell culture inserts with polyethylene terephtalate membranes of 8 µm pore size, free (migration) or covered (invasion) with a film of Matrigel® (Becton Dickinson, France). For easier comparison, results obtained for migration and invasion were normalized to the control condition.

Measurement of intracellular pH - Cells were incubated for 30 min at 37°C in Hank's medium containing 2 µM BCECF-AM (2',7'-bis-(2-carboxyethyl)-5-(and-6)-carboxyfluorescein; excitation 503/440 nm; emission 530 nm). Excess dye was removed by rinsing the cells twice with PSS. H^+ efflux was measured as previously described (Gore et al., 1994).

Membrane fractionation – Membranes were fractionated as described (Calaghan et al., 2008) after extraction in 500 mM Na_2CO_3 (pH 11) containing 0.5 mM EDTA and 1% protease inhibitor cocktail (Sigma-Aldrich). Cells were scrapped then sonicated. Two milliliters homogenate were mixed with an equal volume of 90% sucrose in MES-buffered saline solution (25 mM MES, 150 mM NaCl, 2 mM EDTA, pH 6.5) to form a 45% sucrose solution. A discontinuous sucrose gradient was created by layering onto this a further 4 mL each of 35% and 5% sucrose solutions (MES-buffered saline with 250 mM Na_2CO_3). Gradients were centrifuged for 17 hours at 280,000 x g at 4°C, after which a total of 12 fractions (1 mL each) were collected. Caveolin 1 (Cav1) was used as a marker for the identification of caveolae fractions and β-adaptin was used as a marker for non-lipid raft fractions. Both markers were measured by western blotting following SDS-PAGE. Equal volumes of fractions were loaded onto the gel.

Western Blots - Cells were lysed in presence of 5% SDS and protease inhibitors in PBS. Protein samples were prepared under reducing conditions, separated according to standard SDS-PAGE protocols on polyacrylamide gels (Laemmli, 1970), then transferred onto a PVDF membrane (Millipore, USA). Primary antibodies used were: mouse anti-NHE1 (1/1,500, Chemicon International), mouse anti-HSC70 (1/30,000, TebuBio), rabbit anti-caveolin 1 (1/1,000, BD Biosciences), rabbit anti-β-adaptin (1/2,500, BD Biosciences), rabbit anti-human $Na_V1.5$ (1/200) generated as previously described (Xu et al., 2005) or mouse $PanNa_V$ antibodies (1/200, Sigma Aldrich). Secondary HRP-conjugated antibodies were: goat anti-mouse (1/3,000, TebuBio), goat anti-rabbit (1/5,000, TebuBio), rabbit anti-β-actin-HRP (1/1,000, TebuBio). Densitometric analyses were performed using QuantityOne software v4.6.3 (BioRad, USA).

Immunofluorescence experiments – Cells were cultured for 24h on glass coverslips covered with Matrigel®, then fixed for 15 min in 4% paraformaldehyde and permeabilized for 3 min in 0.1% triton-X-100 in PBS at room temperature. Unspecific sites were saturated by incubating 20 min with 3% bovine serum albumin (BSA) in PBS. Human $Na_V1.5$ channels were detected by incubating cells overnight with anti-$Na_V1.5$ (1/70) in PBS containing 1% BSA. NHE1 were detected using a goat anti-NHE1 (1/100). Cells were washed 3 times in PBS and incubated for 60 min with an anti-rabbit TexasRed (1/800) for $Na_V1.5$ and an anti-goat AlexaFluor488 secondary antibody (1/10,000) for NHE1. Gelatinolytic activity was assessed by culturing cells for 24h in a 3D Matrigel® matrix containing 25 µg/mL of DQ-Gelatin® as previously reported (Gillet et al., 2009). Epifluorescence microscopy was performed with a Nikon TI-S (France). Fluorescence density was quantified by image analysis by ImageJ software 1.38I.

Statistical analyses - Data are displayed as mean ± standard error of the mean (n = number of cells/experiments). One-way ANOVA on ranks followed by a Student-Newmann-Keuls test were used to compare different conditions for cell invasiveness and H^+ efflux. T-tests were used to compare western blot and fluorescence quantifications and results from Q-PCR experiments. Alternatively, Mann-Whitney rank sum test was used when the variance homogeneity test failed.

Statistical significance is indicated as: *, p <0.05; **, p<0.01 and ***, p<0.001. NS stands for not statistically different.

Conflict of interest

Authors declare no conflict of interest.

Acknowledgements

References

Bourguignon, L.Y., Singleton, P.A., Diedrich, F., Stern, R. & Gilad, E. (2004). *J Biol Chem*, **279,** 26991-7007.

Busco, G., Cardone, R.A., Greco, M.R., Bellizzi, A., Colella, M., Antelmi, E., Mancini, M.T., Dell'aquila, M.E., Casavola, V., Paradiso, A. & Reshkin, S.J. (2010). *Faseb J.*

Calaghan, S., Kozera, L. & White, E. (2008). *J Mol Cell Cardiol*, **45,** 88-92.

Cardone, R.A., Casavola, V. & Reshkin, S.J. (2005). *Nat Rev Cancer*, **5,** 786-95.

Diaz, D., Delgadillo, D.M., Hernandez-Gallegos, E., Ramirez-Dominguez, M.E., Hinojosa, L.M., Ortiz, C.S., Berumen, J., Camacho, J. & Gomora, J.C. (2007). *J Cell Physiol*, **210,** 469-78.

Egeblad, M. & Werb, Z. (2002). *Nat Rev Cancer*, **2,** 161-74.

Fraser, S.P., Diss, J.K., Chioni, A.M., Mycielska, M.E., Pan, H., Yamaci, R.F., Pani, F., Siwy, Z., Krasowska, M., Grzywna, Z., Brackenbury, W.J., Theodorou, D., Koyuturk, M., Kaya, H., Battaloglu, E., De Bella, M.T., Slade, M.J., Tolhurst, R., Palmieri, C., Jiang, J., Latchman, D.S., Coombes, R.C. & Djamgoz, M.B. (2005). *Clin Cancer Res*, **11,** 5381-9.

Gatenby, R.A., Smallbone, K., Maini, P.K., Rose, F., Averill, J., Nagle, R.B., Worrall, L. & Gillies, R.J. (2007). *Br J Cancer*, **97,** 646-53.

Gillet, L., Roger, S., Besson, P., Lecaille, F., Gore, J., Bougnoux, P., Lalmanach, G. & Le Guennec, J.Y. (2009). *J Biol Chem*, **284,** 8680-91.

Giusti, I., D'Ascenzo, S., Millimaggi, D., Taraboletti, G., Carta, G., Franceschini, N., Pavan, A. & Dolo, V. (2008). *Neoplasia*, **10,** 481-8.

Gore, J., Besson, P., Hoinard, C. & Bougnoux, P. (1994). *Am J Physiol*, **266,** C110-20.

Gupta, G.P. & Massague, J. (2006). *Cell*, **127,** 679-95.

Kraus, M. & Wolf, B. (1996). *Tumour Biol*, **17,** 133-54.

Laemmli, U.K. (1970). *Nature*, **227,** 680-5.

Laniado, M.E., Lalani, E.N., Fraser, S.P., Grimes, J.A., Bhangal, G., Djamgoz, M.B. & Abel, P.D. (1997). *Am J Pathol*, **150,** 1213-21.

Martinez-Zaguilan, R., Seftor, E.A., Seftor, R.E., Chu, Y.W., Gillies, R.J. & Hendrix, M.J. (1996). *Clin Exp Metastasis*, **14,** 176-86.

Moellering, R.E., Black, K.C., Krishnamurty, C., Baggett, B.K., Stafford, P., Rain, M., Gatenby, R.A. & Gillies, R.J. (2008). *Clin Exp Metastasis*, **25,** 411-25.

Mohamed, M.M. & Sloane, B.F. (2006). *Nat Rev Cancer*, **6,** 764-75.

Parkin, D.M., Bray, F., Ferlay, J. & Pisani, P. (2005). *CA Cancer J Clin*, **55,** 74-108.

Roger, S., Besson, P. & Le Guennec, J.Y. (2003). *Biochim Biophys Acta*, **1616,** 107-11.

Roger, S., Potier, M., Vandier, C., Besson, P. & Le Guennec, J.Y. (2006). *Curr Pharm Des*, **12,** 3681-95.

Roger, S., Rollin, J., Barascu, A., Besson, P., Raynal, P.I., Iochmann, S., Lei, M., Bougnoux, P., Gruel, Y. & Le Guennec, J.Y. (2007). *Int J Biochem Cell Biol*, **39,** 774-86.

Rozhin, J., Sameni, M., Ziegler, G. & Sloane, B.F. (1994). *Cancer Res*, **54,** 6517-25.

Stock, C. & Schwab, A. (2009). *Pflugers Arch*, **458,** 981-92.

Tekpli, X., Huc, L., Lacroix, J., Rissel, M., Poet, M., Noel, J., Dimanche-Boitrel, M.T., Counillon, L. & Lagadic-Gossmann, D. (2008). *J Cell Physiol*, **216,** 207-20.

Xu, S.Z., Zeng, F., Lei, M., Li, J., Gao, B., Xiong, C., Sivaprasadarao, A. & Beech, D.J. (2005). *Nat Biotechnol*, **23,** 1289-93.

Yamaguchi, H., Takeo, Y., Yoshida, S., Kouchi, Z., Nakamura, Y. & Fukami, K. (2009). *Cancer Res*, **69,** 8594-602.

Figure legends

Figure 1: *NHE1 controls H$^+$ efflux in MDA-MB-231 breast cancer cells*. **A,** Representative intracellular pH evolution in NH$_4$Cl-acidified cells resuspended in 130 mM NaCl (NaCl) in presence of 100 nM bafilomycin (Bafilo), 10 µM EIPA or not (control). **B,** Relative H$^+$ efflux measurements after resuspending cells in the same conditions as in A. **C,** Relative H$^+$ efflux measurements after NH$_4$Cl-induced intracellular acidification and resuspension in different extracellular solutions containing: 130 mM NaCl (NaCl) ; 65 mM Na$_2$SO$_4$; 130 mM Choline-Cl (CholineCl); 130 mM N-methyl-D-glucamine (NMDG-Cl); 20 mM NaHCO$_3$ + 110 mM NaCl in presence or not of 100 µM 4,4'-diisothiocyanato-stilbene-2,2'-disulfonic acid (DIDS) (n=2-12). **D,** Representative western blots showing NHE1, HSC-70 and β-actin from MDA-MB-231 cells transfected with control siRNA (siCTL) or with siRNA specific for NHE1 (siNHE1) (n=4). **E,** Relative H$^+$ efflux from cells transfected with siCTL or with siNHE1, in presence of 10 µM EIPA or not (n= 4).
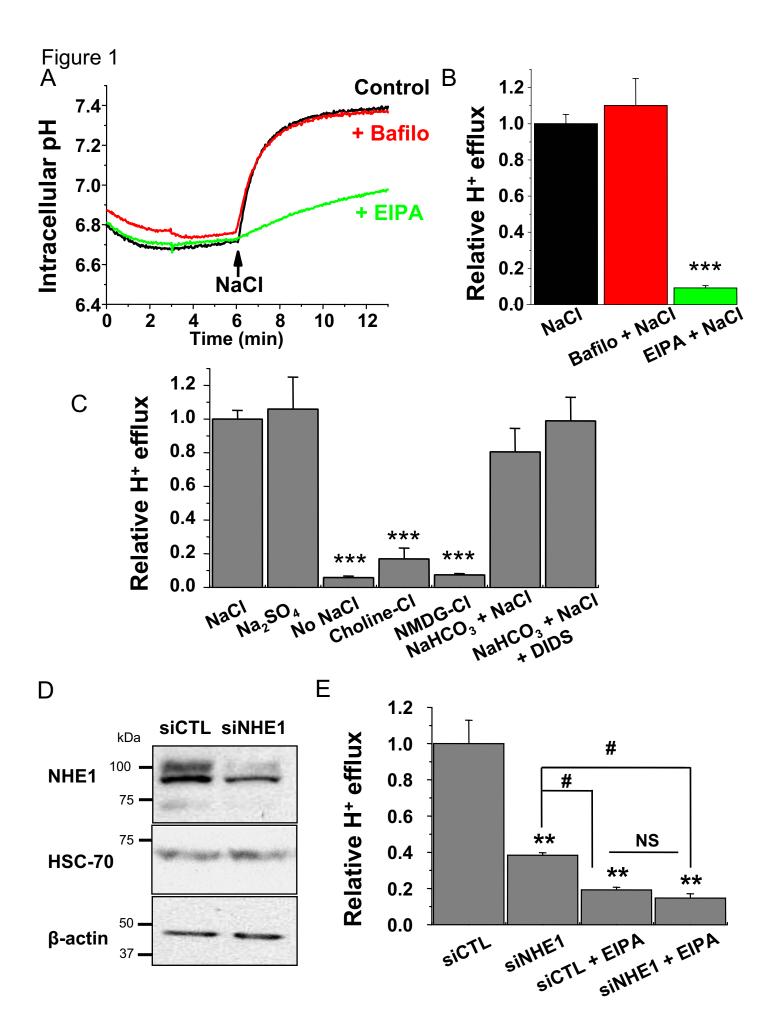
Figure 2: *Na$_V$1.5 activity enhances H$^+$ efflux and invasiveness of breast cancer cells*. **A**, RT-PCR experiments showing the mRNA expression of Na$_V$1.5, NHE1 and 18S RNA in MDA-MB-231 and MCF-7 breast cancer cells, and MCF-10A non-cancer cells (n= 2). **B**, Representative current-voltage protocols, obtained from the same cell lines as in A, from a holding potential of -70 mV to +90 mV, with 10 mV increments. The arrow indicates the voltage-gated sodium current. **C**, Representative western blots of Na$_V$1.5, NHE1, HSC-70 and β-actin performed on MDA-MB-231 cells transfected with control siRNA (siCTL) or with siRNA specific for Na$_V$1.5 (siNa$_V$1.5) (n= 4). **D**, Representative sodium currents recorded from a holding potential of -100 mV to -5 mV in physiological saline solution (PSS), or in presence of EIPA (10 µM), TTX (30 µM) or when cells were transfected with siNa$_V$1.5. **E**, Relative H$^+$ efflux, calculated using the BCECF probe, after NH$_4$Cl-induced intracellular acidification, from MDA-MB-231 cells transfected with siCTL or with
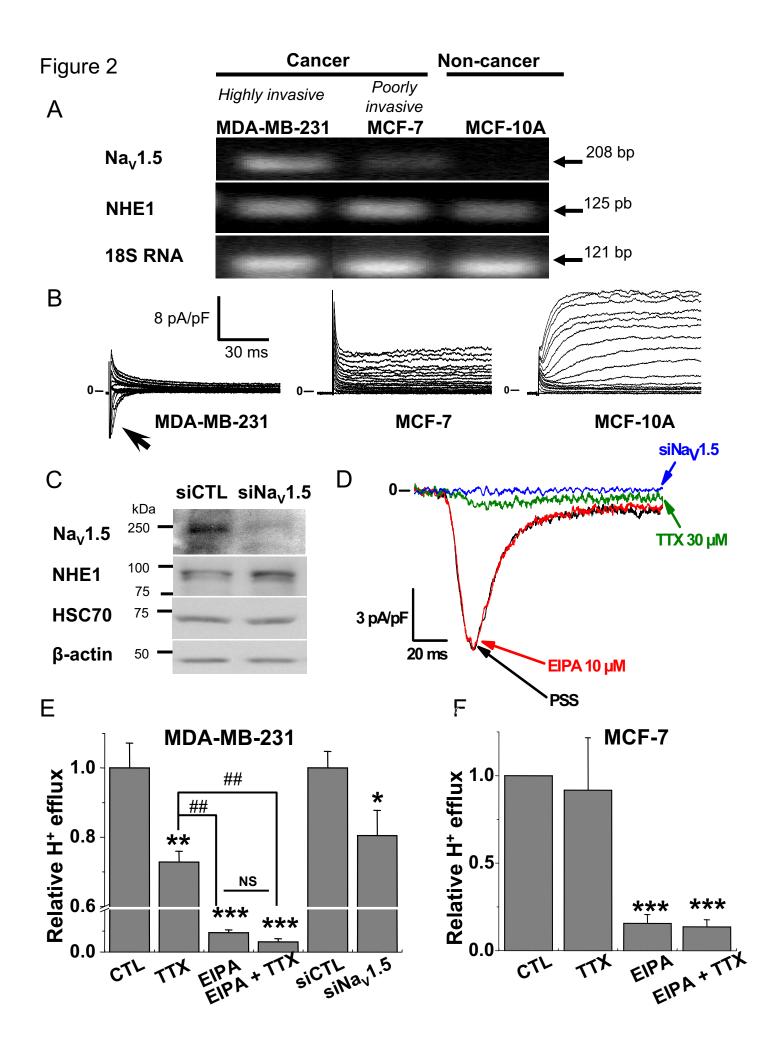
siNa$_V$1.5, in presence of 30 µM TTX, 10 µM EIPA or not (CTL) (n= 9-11). **F**, Relative H$^+$ efflux from MCF-7 cells in presence of 30 µM TTX and/or 10 µM EIPA or none (CTL) (n= 3).
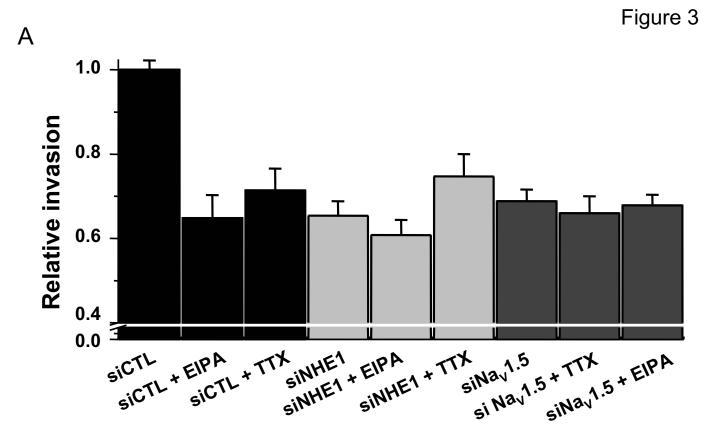
Figure 3: *Na$_V$1.5 enhances cancer cell invasiveness through the regulation of NHE1 function*. **A,** Relative matrix invasion by MDA-MB-231 breast cancer cells transfected with siCTL, siNa$_V$1.5 or siNHE1 in presence or absence of EIPA (1 µM) or TTX (30 µM) (n= 4). All conditions tested were statistically different from siCTL condition at p<0.001 but there was no significant difference between treatments. **B**, Fluorescence imaging of cells grown for 24 h within a 3D Matrigel® matrix containing DQ-Gelatin® in control conditions (CTL), in presence of 30 µM TTX (TTX), 1 µM EIPA (EIPA) or a combination of both (EIPA+TTX). **C**, Quantification of fluorescence intensity from DQ-gelatin cleavage expressed as a percentage of the control condition (n=11-17).
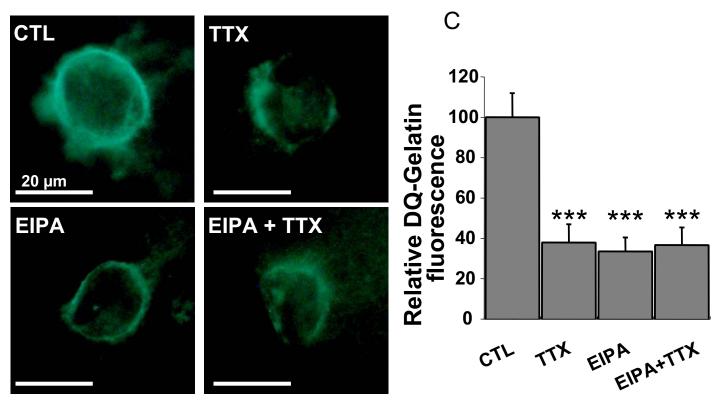
Figure 4: *Na$_V$1.5 and NHE1 colocalize in caveolin-rich membrane rafts*. **A**, Representative immunofluorescence staining performed on a MDA-MB-231 cell cultured on Matrigel®, using primary antibodies specific for NHE1 or Na$_V$1.5, and DAPI for nucleus staining. **B**, Membrane fractionation on a sucrose gradient shows that NHE1 and Na$_V$ channels are colocalized in buoyant fraction number 5. This fraction represents caveolae-containing membranes as shown by enrichment in Caveolin-1 (Cav1). β-adaptin was used as a marker of non-raft fractions.
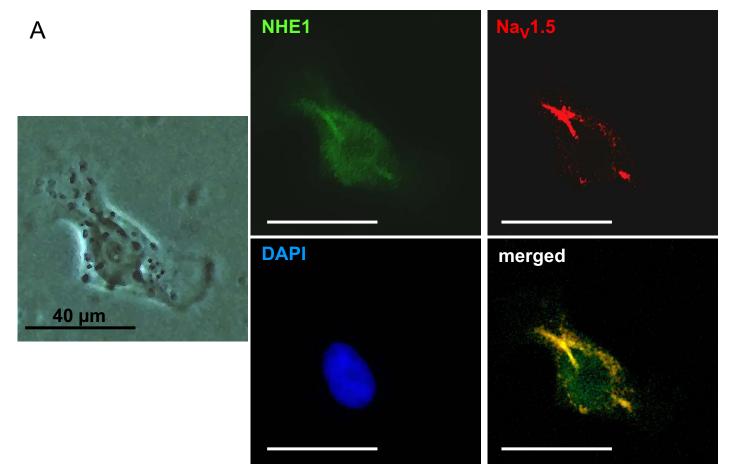
Figure 1

Figure 2

A

Cancer
Highly invasive   Poorly invasive
MDA-MB-231   MCF-7   MCF-10A   Non-cancer

$Na_V1.5$ ← 208 bp
NHE1 ← 125 pb
18S RNA ← 121 bp

B

8 pA/pF
30 ms

MDA-MB-231   MCF-7   MCF-10A

C

siCTL $siNa_V1.5$
kDa
$Na_V1.5$ 250
NHE1   100   75
HSC70   75
β-actin   50

D

0 —
$siNa_V1.5$
TTX 30 µM
EIPA 10 µM
PSS
3 pA/pF
20 ms

E

MDA-MB-231

Relative H^+ efflux

1.0   0.8   0.6   0.0

CTL   TTX   EIPA   EIPA + TTX   siCTL $siNa_V1.5$

** ## ## NS *** *** *

F

MCF-7

Relative H^+ efflux

1.0   0.5   0.0
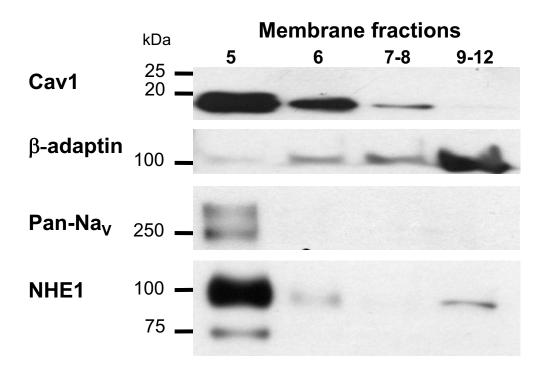
CTL   TTX   EIPA   EIPA + TTX

*** ***

Figure 3

Figure 4

A

B

Supplementary Figure legends

Supplementary figure 1 :

A, Dose-response curve of EIPA on H^+ efflux from MDA-MB-231 calculated as explained in Methods section using the BCECF probe after NH_4Cl-induced intracellular acidification. The IC_{50} obtained from the sigmoidal fit was 0.11 ± 0.02 µM. **B**, Mean data from western blot analyses showing the NHE1 protein expression relative to HSC-70 expression from MDA-MB-231 cancer cells transfected with siRNA against NHE1 (siNHE1) *vs*. control (siCTL) (n= 4). The two bands were corresponding to the glycosylated and non-glycosylated forms were quantified as a whole. **C**, $Na_V1.5$ mRNA expression assessed by Q-PCR in MDA-MB-231 cells transfected with siRNA against $Na_V1.5$ (si$Na_V1.5$) *vs*. control (siCTL) (n= 2 experiments). **D**, $Na_V1.5$ mRNA expression assessed by Q-PCR in MDA-MB-231 cells transfected with siRNA against NHE1 (siNHE1) *vs*. control (siCTL) (n= 3). **E**, Current-voltage relationship of the sodium current obtained from a holding potential of -100 mV in PSS from MDA-MB-231 cells transfected with siNHE1 (red circles, n= 16 cells) or with siCTL (black squares, n= 13 cells). **F**, Conductance-(■) and availability-(●) voltage relationships obtained from MDA-MB-231 cells transfected with siNHE1 (red symbol, n= 16 cells) or with siCTL (black symbol, n= 13 cells). Sigmoidal fits of these relationships gives $V_{1/2}$-conductance of -27.9 ± 0.9 mV and -30.1 ± 0.2 mV for siCTL and siNHE1 respectively. $V_{1/2}$-availability were -68.0 ± 1.7 mV and -66.8 ± 1.5 mV for siCTL and siNHE1 respectively. No statistical difference was found.

Statistically different versus control condition at: ***p<0.001.

Supplementary Figure 1